# Supplementary material for LHCb-PAPER-2017-002

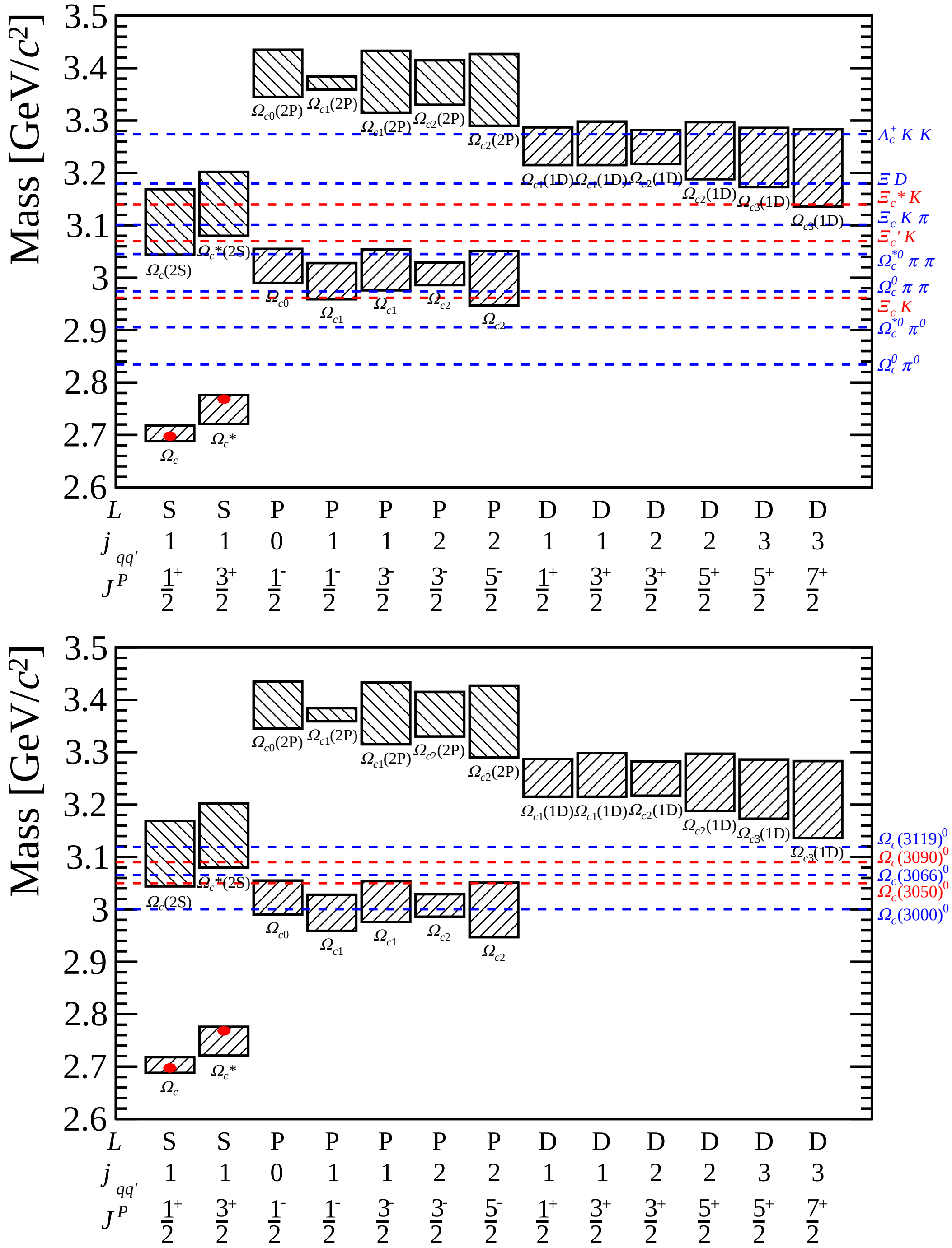


Figure 1: Mass predictions of the excited $\Omega_c^0$ states [1–7]. The boxes cover the range of predictions for the masses of each state, and the red dots indicate the measured values. The x-axis reports the quantum numbers of the excited $\Omega_c^0$ states: the orbital angular momentum ($L$), the total angular momentum of the light diquark ($j_{qq'}$), and the spin-parity of the excited $\Omega_c^0$ state ($J^P$). The horizontal lines correspond to (top) the hadronic thresholds of the possible final states, and (bottom) the measured masses of the new $\Omega_c^0$ states. Note that the boxes and red dots are identical in the top and bottom figures.

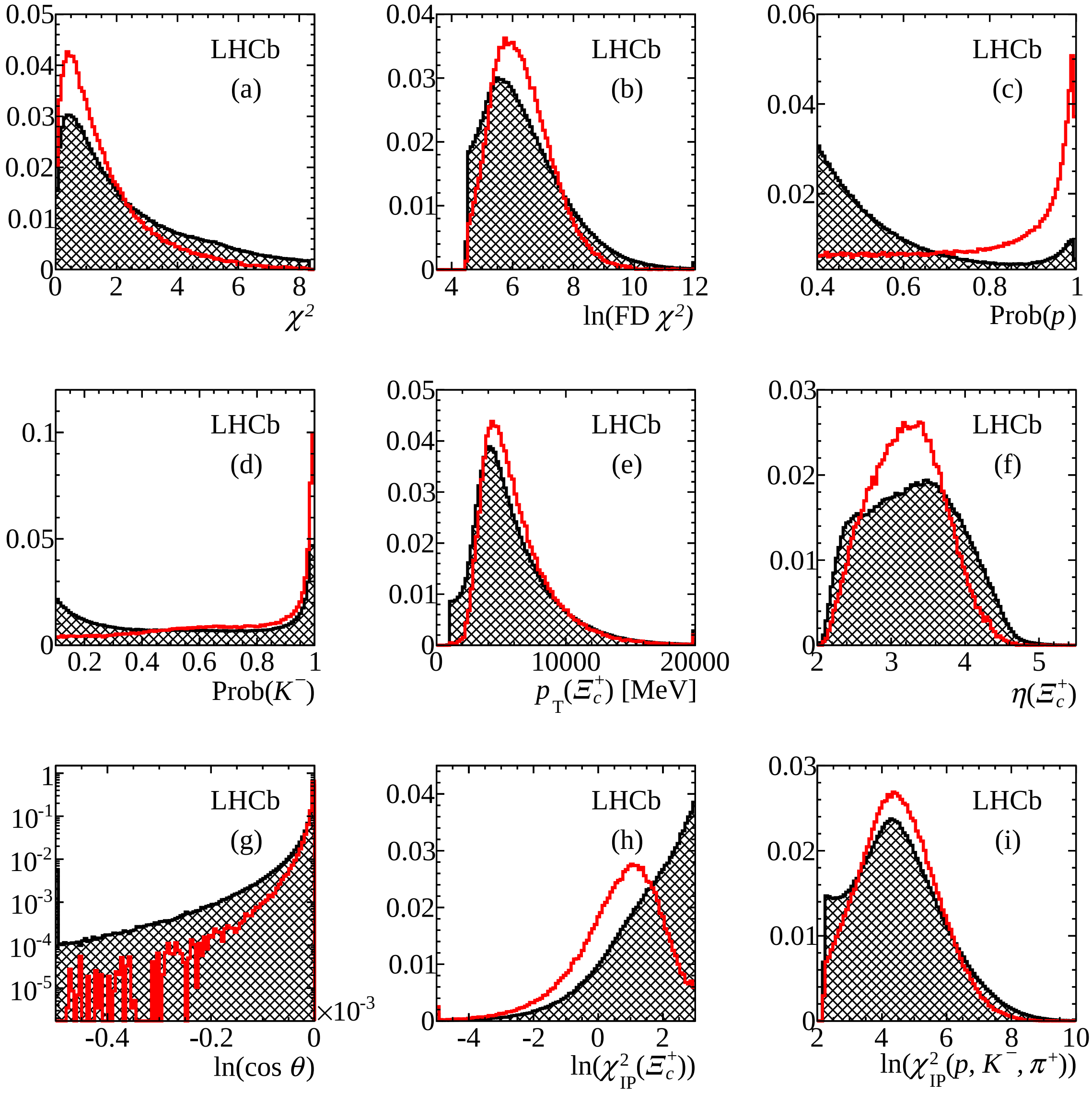


Figure 2: Normalized probability distribution functions for signal (solid red) and background events (hatched black) used in a likelihood-ratio test for the event selection of $\Xi_c^+ \to pK^-\pi^+$ (2012 data): (a) vertex fit $\chi^2$, (b) logarithm of the flight distance significance in units of $\chi^2$ with respect to the primary vertex (c) proton identification probability returned by a neural-net algorithm, (d) kaon identification probability returned by a neural-net algorithm, (e) transverse momentum of the $\Xi_c^+$ candidate, (f) pseudorapidity of the $\Xi_c^+$ candidate, (g) logarithm of the cosine of the angle between the $\Xi_c^+$ momentum and the direction vector from the primary vertex to $\Xi_c^+$ decay vertex, (h) logarithm of $\chi^2_{\rm IP}$ of the $\Xi_c^+$ candidate, (i) logarithm of $\chi^2_{\rm IP}$ of each track, The $\chi^2_{\rm IP}$ is defined as the difference between the $\chi^2$ of the primary vertex reconstructed with and without the candidate in question. Figure (i) is obtained by summing the distributions of the protons, pions and kaons; the same PDF is used for each of these candidates.

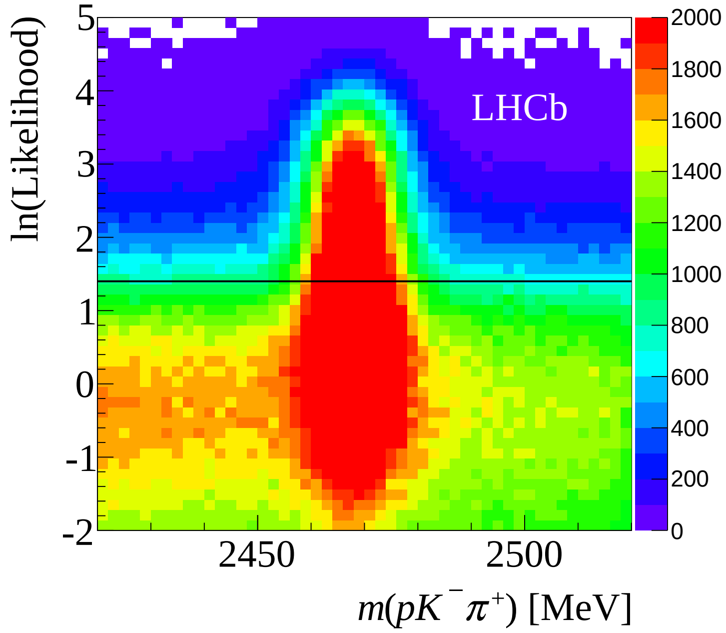


Figure 3: Two-dimensional distribution of $\Xi_c^+$ candidates, as a function of the $pK^-\pi^+$ mass (horizontal) and the output of the likelihood ratio test (vertical) (2012 data). The horizontal line corresponds to the criterion applied for the selection of the $\Xi_c^+ \to pK^-\pi^+$ candidates.

Table 1: Systematic uncertainties on the masses and widths of the new $\Omega_c^0$ states in units of MeV.

| Source | $\Omega_c(3000)^0$ $(m, \Gamma)$ | $\Omega_c(3050)^0$ $(m, \Gamma)$ | $\Omega_c(3066)^0$ $(m, \Gamma)$ | $\Omega_c(3090)^0$ $(m, \Gamma)$ | $\Omega_c(3119)^0$ $(m, \Gamma)$ | $\Omega_c(3188)^0$ $(m, \Gamma)$ |
|---|---|---|---|---|---|---|
| Fit bias | (0.00, 0.10) | (0.03, 0.00) | (0.01, 0.00) | (0.04, 0.00) | (0.00, 0.00) | (0.55, 0.00) |
| Background model | (0.03, 0.25) | (0.00, 0.05) | (0.00, 0.10) | (0.00, 0.49) | (0.01, 0.21) | (1.81, 4.92) |
| Interference | (0.05, 0.09) | (0.09, 0.08) | (0.27, 0.15) | (0.48, 0.49) | (0.89, 0.17) | (8.19, 6.56) |
| Feed-down shift | (0.13, 0.09) | (0.00, 0.02) | (0.00, 0.03) | (0.00, 0.09) | (0.00, 0.03) | (0.21, 0.82) |
| Mass scale at 7–8 TeV | (0.01, 0.00) | (0.03, 0.00) | (0.03, 0.00) | (0.04, 0.00) | (0.05, 0.00) | (0.07, 0.00) |
| Mass scale at 13 TeV | (0.00, 0.00) | (0.01, 0.00) | (0.01, 0.00) | (0.01, 0.00) | (0.02, 0.00) | (0.02, 0.00) |
| Data-MC discrepancy | (0.00, 0.08) | (0.00, 0.01) | (0.00, 0.06) | (0.00, 0.15) | (0.00, 0.02) | (0.00, 0.00) |
| High-mass description | (0.00, 0.11) | (0.00, 0.00) | (0.00, 0.03) | (0.10, 0.37) | (0.00, 0.30) | (9.50, 7.20) |
| Total | (0.14, 0.31) | (0.10, 0.10) | (0.27, 0.19) | (0.48, 0.80) | (0.89, 0.40) | (12.7, 10.9) |

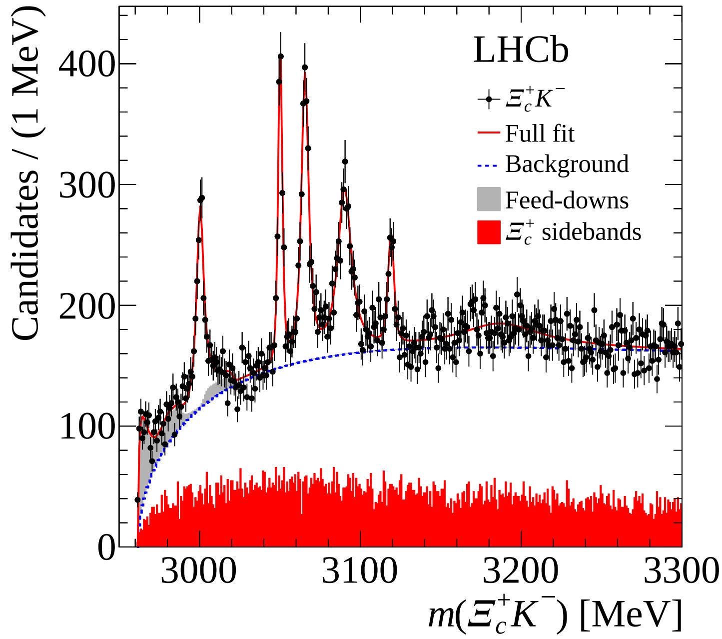


Figure 4: Distribution of the reconstructed invariant mass $m(\Xi_c^+ K^-)$ for all candidates passing the likelihood ratio selection; the solid (red) curve shows the result of the fit, and the dashed (blue) line indicates the fitted background. The shaded (red) histogram shows the corresponding mass spectrum from the $\Xi_c^+$ sidebands and the shaded (light gray) distributions indicate the feed-down from partially reconstructed $\Omega_c(X)^0$ resonances.

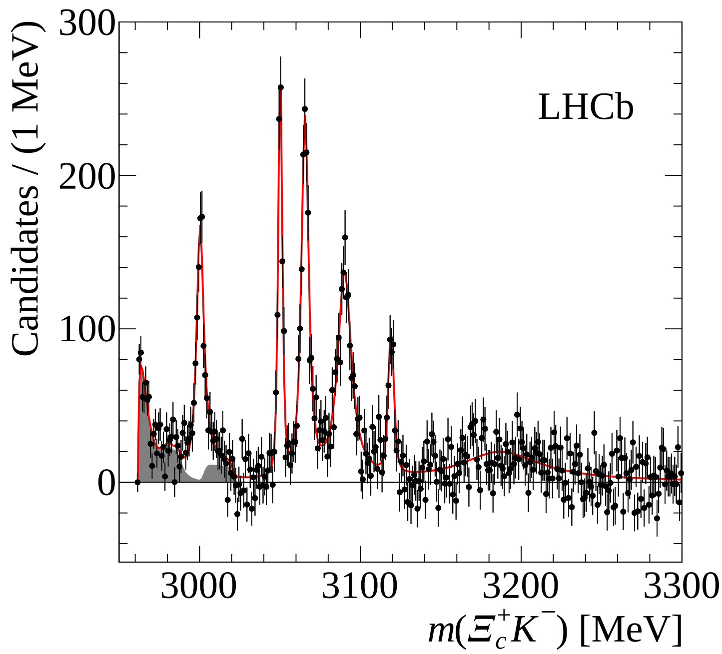


Figure 5: Background-subtracted $m(\Xi_c^+ K^-)$ mass spectrum; the solid (red) curve is the result from the fit, and the (gray) shaded distributions indicate the feed-down from partially reconstructed $\Omega_c(X)^0$ resonances.

# References


[1] D. Ebert, R. N. Faustov, and V. O. Galkin, *Masses of excited heavy baryons in the relativistic quark-diquark picture*, Phys. Lett. **B659** (2008) 612, arXiv:0705.2957.

[2] W. Roberts and M. Pervin, *Heavy baryons in a quark model*, Int. J. Mod. Phys. **A23** (2008) 2817, arXiv:0711.2492.

[3] H. Garcilazo, J. Vijande, and A. Valcarce, *Faddeev study of heavy-baryon spectroscopy*, J. Phys. **G34** (2007) 961, arXiv:hep-ph/0703257.

[4] S. Migura, D. Merten, B. Metsch, and H.-R. Petry, *Charmed baryons in a relativistic quark model*, Eur. Phys. J. **A28** (2006) 41, arXiv:hep-ph/0602153.

[5] D. Ebert, R. N. Faustov, and V. O. Galkin, *Spectroscopy and Regge trajectories of heavy baryons in the relativistic quark-diquark picture*, Phys. Rev. **D84** (2011) 014025, arXiv:1105.0583.

[6] A. Valcarce, H. Garcilazo, and J. Vijande, *Towards an understanding of heavy baryon spectroscopy*, Eur. Phys. J. **A37** (2008) 217, arXiv:0807.2973.

[7] Z. Shah, K. Thakkar, A. K. Rai, and P. C. Vinodkumar, *Mass spectra and Regge trajectories of $\Lambda_c^+$, $\Sigma_c^0$, $\Xi_c^0$ and $\Omega_c^0$ baryons*, Chin. Phys. **C40** (2016) 123102, arXiv:1609.08464.